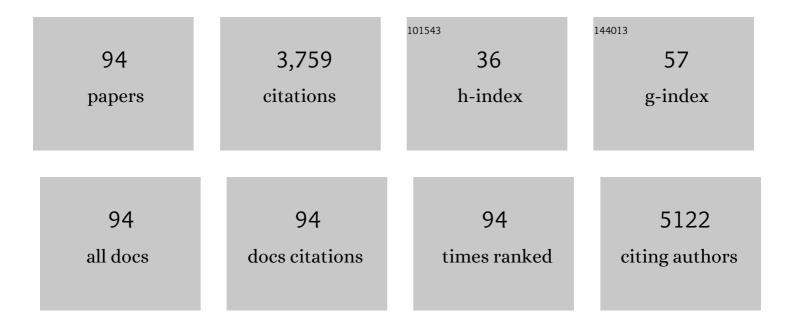
Zhao-Jie Wang

List of Publications by Year in descending order

Source: https://exaly.com/author-pdf/5495299/publications.pdf Version: 2024-02-01



#	Article	IF	CITATIONS
1	Ultrasensitive Hydrogen Sensor Based on Pd ⁰ -Loaded SnO ₂ Electrospun Nanofibers at Room Temperature. ACS Applied Materials & Interfaces, 2013, 5, 2013-2021.	8.0	181
2	Improved Hydrogen Monitoring Properties Based on p-NiO/n-SnO ₂ Heterojunction Composite Nanofibers. Journal of Physical Chemistry C, 2010, 114, 6100-6105.	3.1	158
3	A highly sensitive and fast-responding sensor based on electrospun In2O3 nanofibers. Sensors and Actuators B: Chemical, 2009, 142, 61-65.	7.8	155
4	A highly sensitive ethanol sensor based on mesoporous ZnO–SnO ₂ nanofibers. Nanotechnology, 2009, 20, 075501.	2.6	148
5	Synthesis of few-layer 1T′-MoTe ₂ ultrathin nanosheets for high-performance pseudocapacitors. Journal of Materials Chemistry A, 2017, 5, 1035-1042.	10.3	134
6	Construction of multi-dimensional core/shell Ni/NiCoP nano-heterojunction for efficient electrocatalytic water splitting. Applied Catalysis B: Environmental, 2019, 259, 118039.	20.2	124
7	Enhancement of hydrogen monitoring properties based on Pd–SnO2 composite nanofibers. Sensors and Actuators B: Chemical, 2010, 147, 111-115.	7.8	117
8	Strategies to enhance CO ₂ capture and separation based on engineering absorbent materials. Journal of Materials Chemistry A, 2015, 3, 12118-12132.	10.3	98
9	Adsorption of Cu(II) from aqueous solution by anatase mesoporous TiO2 nanofibers prepared via electrospinning. Journal of Colloid and Interface Science, 2012, 367, 429-435.	9.4	92
10	Humidity sensor based on LiCl-doped ZnO electrospun nanofibers. Sensors and Actuators B: Chemical, 2009, 141, 404-409.	7.8	88
11	Catalyzing zinc-ion intercalation in hydrated vanadates for aqueous zinc-ion batteries. Journal of Materials Chemistry A, 2020, 8, 7713-7723.	10.3	84
12	Assembly of Pt nanoparticles on electrospun In2O3 nanofibers for H2S detection. Journal of Colloid and Interface Science, 2009, 338, 366-370.	9.4	77
13	Effects of Al doping on SnO2 nanofibers in hydrogen sensor. Sensors and Actuators B: Chemical, 2011, 160, 858-863.	7.8	76
14	Carbon quantum dot-induced self-assembly of ultrathin Ni(OH)2 nanosheets: A facile method for fabricating three-dimensional porous hierarchical composite micro-nanostructures with excellent supercapacitor performance. Nano Research, 2017, 10, 3005-3017.	10.4	73
15	Architecting a Mesoporous N-Doped Graphitic Carbon Framework Encapsulating CoTe ₂ as an Efficient Oxygen Evolution Electrocatalyst. ACS Applied Materials & Interfaces, 2017, 9, 36146-36153.	8.0	73
16	Synergic effect within n-type inorganic–p-type organic nano-hybrids in gas sensors. Journal of Materials Chemistry C, 2013, 1, 3017.	5.5	70
17	Initiating an efficient electrocatalyst for water splitting via valence configuration of cobalt-iron oxide. Applied Catalysis B: Environmental, 2019, 258, 117968.	20.2	70
18	Can N, S Cocoordination Promote Single Atom Catalyst Performance in CO ₂ RR?	10.0	62

 $^{18 \}qquad Fea \in \mathbb{N} < sub > 2 < /sub > S < sub > 2 < /sub > Normalize in Co (sub > 2 < /sub > Normalize in Co (sub > 2 < /sub > Normalize in Co (sub > 2 < /sub > Normalize in Co (sub > 2 < /sub > Normalize in Co (sub > 2 < /sub > Normalize in Co (sub > 2 < /sub > Normalize in Co (sub > 2 < /sub > Normalize in Co (sub > 2 < /sub > Normalize in Co (sub > 2 < /sub > 2 < /sub > 10.0 62$

#	Article	IF	CITATIONS
19	Ni Foam-Supported Carbon-Sheathed NiMoO ₄ Nanowires as Integrated Electrode for High-Performance Hybrid Supercapacitors. ACS Sustainable Chemistry and Engineering, 2017, 5, 5964-5971.	6.7	61
20	Initial Reduction of CO ₂ on Pd-, Ru-, and Cu-Doped CeO ₂ (111) Surfaces: Effects of Surface Modification on Catalytic Activity and Selectivity. ACS Applied Materials & Interfaces, 2017, 9, 26107-26117.	8.0	61
21	1T@2H-MoSe2 nanosheets directly arrayed on Ti plate: An efficient electrocatalytic electrode for hydrogen evolution reaction. Nano Research, 2018, 11, 4587-4598.	10.4	56
22	Contemporaneous inverse manipulation of the valence configuration to preferred Co2+ and Ni3+ for enhanced overall water electrocatalysis. Applied Catalysis B: Environmental, 2021, 284, 119725.	20.2	55
23	Auâ€Doped Polyacrylonitrile–Polyaniline Core–Shell Electrospun Nanofibers Having High Fieldâ€Effect Mobilities. Small, 2011, 7, 597-600.	10.0	54
24	Cu acting as Fe activity promoter in dual-atom Cu/Fe-NC catalyst in CO2RR to C1 products. Applied Surface Science, 2021, 564, 150423.	6.1	52
25	Electrochemical determination of dopamine based on electrospun CeO2/Au composite nanofibers. Electrochimica Acta, 2013, 95, 12-17.	5.2	50
26	Fabrication of novel Ag nanowires/poly(vinylidene fluoride) nanocomposite film with high dielectric constant. Physica Status Solidi (A) Applications and Materials Science, 2010, 207, 1870-1873.	1.8	49
27	Penta-graphene as a promising controllable CO2 capture and separation material in an electric field. Applied Surface Science, 2020, 502, 144067.	6.1	49
28	Interlayer expanded lamellar CoSe 2 on carbon paper as highly efficient and stable overall water splitting electrodes. Electrochimica Acta, 2017, 241, 106-115.	5.2	48
29	Coupled Heterostructure of Mo–Fe Selenide Nanosheets Supported on Carbon Paper as an Integrated Electrocatalyst for Efficient Hydrogen Evolution. ACS Applied Materials & Interfaces, 2018, 10, 27787-27794.	8.0	46
30	Concaving AgI sub-microparticles for enhanced photocatalysis. Nano Energy, 2014, 9, 204-211.	16.0	45
31	Lamellar structured CoSe 2 nanosheets directly arrayed on Ti plate as an efficient electrochemical catalyst for hydrogen evolution. Electrochimica Acta, 2016, 217, 156-162.	5.2	45
32	Sulfonated Poly(ether ether ketone)/Polypyrrole Core–Shell Nanofibers: A Novel Polymeric Adsorbent/Conducting Polymer Nanostructures for Ultrasensitive Gas Sensors. ACS Applied Materials & Interfaces, 2012, 4, 6080-6084.	8.0	44
33	Mechanistic insights into porous graphene membranes for helium separation and hydrogen purification. Applied Surface Science, 2018, 441, 631-638.	6.1	42
34	Hierarchical self-supported C@TiO2-MoS2 core-shell nanofiber mats as flexible anode for advanced lithium ion batteries. Applied Surface Science, 2017, 423, 375-382.	6.1	40
35	Rational Design of Metallic NiTe _{<i>x</i>} (<i>x</i> = 1 or 2) as Bifunctional Electrocatalysts for Efficient Urea Conversion. ACS Applied Energy Materials, 2019, 2, 3363-3372.	5.1	40
36	Oneâ€Dimensional Polyelectrolyte/Polymeric Semiconductor Core/Shell Structure: Sulfonated Poly(arylene ether ketone)/Polyaniline Nanofibers for Organic Fieldâ€Effect Transistors. Advanced Materials, 2011, 23, 5109-5112.	21.0	39

#	Article	IF	CITATIONS
37	Stimulus-responsive adsorbent materials for CO ₂ capture and separation. Journal of Materials Chemistry A, 2020, 8, 10519-10533.	10.3	39
38	A general approach to 3D porous CQDs/MxOy (M = Co, Ni) for remarkable performance hybrid supercapacitors. Chemical Engineering Journal, 2017, 326, 58-67.	12.7	37
39	The synthesis of hollow MoS ₂ nanospheres assembled by ultrathin nanosheets for an enhanced energy storage performance. Inorganic Chemistry Frontiers, 2017, 4, 309-314.	6.0	37
40	A facile co-precipitation synthesis of robust FeCo phosphate electrocatalysts for efficient oxygen evolution. Electrochimica Acta, 2018, 264, 244-250.	5.2	36
41	Improved photocatalytic activity of mesoporous ZnO–SnO2 coupled nanofibers. Catalysis Communications, 2009, 11, 257-260.	3.3	35
42	Two Birds with One Stone: Contemporaneously Boosting OER Activity and Kinetics for Layered Double Hydroxide Inspired by Photosystem II. Advanced Functional Materials, 2022, 32, .	14.9	33
43	A Rapidly Responding Sensor for Methanol Based on Electrospun In ₂ O ₃ –SnO ₂ Nanofibers. Journal of the American Ceramic Society, 2010, 93, 15-17.	3.8	32
44	Ethanol chemiresistor with enhanced discriminative ability from acetone based on Sr-doped SnO2 nanofibers. Journal of Colloid and Interface Science, 2015, 437, 252-258.	9.4	32
45	Strain-controlled carbon nitride: A continuously tunable membrane for gas separation. Applied Surface Science, 2020, 506, 144675.	6.1	29
46	Carbon Quantum Dots Promote Coupled Valence Engineering of V ₂ O ₅ Nanobelts for Highâ€Performance Aqueous Zincâ€ion Batteries. ChemSusChem, 2021, 14, 2076-2083.	6.8	29
47	Carbon quantum dots decorated hierarchical Ni(OH)2 with lamellar structure for outstanding supercapacitor. Materials Letters, 2017, 186, 131-134.	2.6	27
48	Direct tuning of meso-/micro-porous structure of carbon nanofibers confining Sb nanocrystals for advanced sodium and potassium storage. Journal of Alloys and Compounds, 2020, 833, 155127.	5.5	27
49	Edge-functionalized nanoporous carbons for high adsorption capacity and selectivity of CO2 over N2. Applied Surface Science, 2017, 410, 259-266.	6.1	25
50	Nanoporous Boron Nitride Membranes for Helium Separation. ACS Applied Nano Materials, 2019, 2, 4471-4479.	5.0	25
51	Interlayer expanded molybdenum disulfide nanosheets assembly for electrochemical supercapacitor with enhanced performance. Materials Chemistry and Physics, 2017, 192, 100-107.	4.0	24
52	Alkyl amine functionalized triphenylamine-based covalent organic frameworks for high-efficiency CO2 capture and separation over N2. Materials Letters, 2018, 230, 28-31.	2.6	24
53	How can the Dualâ€atom Catalyst FeCo–NC Surpass Singleâ€atom Catalysts Fe–NC/Co–NC in CO ₂ RR? – CO Intermediate Assisted Promotion via a Synergistic Effect. Energy and Environmental Materials, 2023, 6, .	12.8	24
54	Ultrafine porous carbon fibers for SO2 adsorption via electrospinning of polyacrylonitrile solution. Journal of Colloid and Interface Science, 2008, 327, 388-392.	9.4	23

#	Article	IF	CITATIONS
55	A Novel Alcohol Detector Based on ZrO ₂ â€Doped SnO ₂ Electrospun Nanofibers. Journal of the American Ceramic Society, 2010, 93, 634-637.	3.8	23
56	Rational design of TiO2@ nitrogen-doped carbon coaxial nanotubes as anode for advanced lithium ion batteries. Applied Surface Science, 2018, 458, 1018-1025.	6.1	22
57	Boosting oxygen evolution reaction of hierarchical spongy NiFe-PBA/Ni3C(B) electrocatalyst: Interfacial engineering with matchable structure. Chemical Engineering Journal, 2022, 433, 133524.	12.7	22
58	Carbon phosphides: promising electric field controllable nanoporous materials for CO ₂ capture and separation. Journal of Materials Chemistry A, 2020, 8, 9970-9980.	10.3	21
59	Composite membranes based on sulfonated poly(aryl ether ketone)s containing the hexafluoroisopropylidene diphenyl moiety and poly(amic acid) for proton exchange membrane fuel cell application. International Journal of Hydrogen Energy, 2011, 36, 14622-14631.	7.1	20
60	A Fast Humidity Sensor Based on Li+-Doped SnO2 One-Dimensional Porous Nanofibers. Materials, 2017, 10, 535.	2.9	20
61	Synthesis of heterostructured Pd@TiO 2 /TiOF 2 nanohybrids with enhanced photocatalytic performance. Materials Research Bulletin, 2016, 80, 337-343.	5.2	19
62	Theoretical investigation on the hydrogen evolution reaction mechanism at MoS ₂ heterostructures: the essential role of the 1T/2H phase interface. Catalysis Science and Technology, 2020, 10, 458-465.	4.1	19
63	Synthesis of layer-expanded MoS2 nanosheets/carbon fibers nanocomposites for electrochemical hydrogen evolution reaction. Materials Chemistry and Physics, 2016, 183, 18-23.	4.0	18
64	In Situ Coupling Reconstruction of Cobalt–Iron Oxide on a Cobalt Phosphate Nanoarray with Interfacial Electronic Features for Highly Enhanced Water Oxidation Catalysis. ACS Sustainable Chemistry and Engineering, 2020, 8, 4773-4780.	6.7	18
65	Li-modified nanoporous carbons for high-performance adsorption and separation of CO2 over N2: A combined DFT and GCMC computational study. Journal of CO2 Utilization, 2018, 26, 588-594.	6.8	17
66	N-type SnO ₂ nanosheets standing on p-type carbon nanofibers: a novel hierarchical nanostructures based hydrogen sensor. RSC Advances, 2015, 5, 64582-64587.	3.6	16
67	CO2 capture and separation over N2 and CH4 in nanoporous MFM-300(In, Al, Ga, and In-3N): Insight from GCMC simulations. Journal of CO2 Utilization, 2018, 28, 145-151.	6.8	16
68	Solar-driven Pt modified hollow structured CdS photocatalyst for efficient hydrogen evolution. RSC Advances, 2014, 4, 36665.	3.6	15
69	Constructing surface vacancy to activate the stuck MXenes for high-performance CO2 reduction reaction. Journal of CO2 Utilization, 2022, 62, 102074.	6.8	15
70	Facile control of surface reconstruction with Co2+ or Co3+-rich (oxy)hydroxide surface on ZnCo phosphate for large-current-density hydrogen evolution in alkali. Materials Today Physics, 2021, 20, 100448.	6.0	14
71	In-situ solution synthesis of graphene supported lamellar 1T'-MoTe 2 for enhanced pseudocapacitors. Materials Letters, 2017, 206, 229-232.	2.6	13
72	Two-dimensional coupling: Sb nanoplates embedded in MoS 2 nanosheets as efficient anode for advanced sodium ion batteries. Materials Chemistry and Physics, 2018, 211, 375-381.	4.0	12

#	Article	IF	CITATIONS
73	Facile synthesis of an antimony-doped Cu/Cu ₂ O catalyst with robust CO production in a broad range of potentials for CO ₂ electrochemical reduction. Journal of Materials Chemistry A, 2021, 9, 23234-23242.	10.3	12
74	Synthesis of 3D flower-like cobalt sulfide hierachitecture for high-performance electrochemical energy storage. Journal of Nanoparticle Research, 2017, 19, 1.	1.9	11
75	Monolith free-standing plasmonic PAN/Ag/AgX (X = Br, I) nanofiber mat as easily recoverable visible-light-driven photocatalyst. Rare Metals, 2019, 38, 361-368.	7.1	11
76	Impact of diverse active sites on MoS2 catalyst: Competition on active site formation and selectivity of thiophene hydrodesulfurization reaction. Molecular Catalysis, 2019, 463, 67-76.	2.0	11
77	High-efficiency CO2 capture and separation over N2 in penta-graphene pores: insights from GCMC and DFT simulations. Journal of Materials Science, 2020, 55, 16603-16611.	3.7	11
78	Triple-atom catalysts 3TM-GYs (TMÂ=ÂCu, Fe, and Co; GYÂ=Âgraphyne) for high-performance CO2 reduction reaction to C1 products. Applied Materials Today, 2021, 25, 101245.	4.3	10
79	Hydrothermal synthesis of ammonium vanadate [(NH4)2V7O16•3.6H2O] as a promising zinc-ion cathode: Experimental and theoretical study of its storage. Electrochimica Acta, 2022, 404, 139785.	5.2	9
80	Theoretical Investigation on Copper(I) Complexes Featuring a Phosphonic Acid Anchor with Asymmetric Ligands for DSSC. ACS Applied Electronic Materials, 2020, 2, 2141-2150.	4.3	8
81	Tracking CO2 capture and separation over N2 in a flexible metal–organic framework: insights from GCMC and DFT simulations. Journal of Materials Science, 2021, 56, 10414-10423.	3.7	8
82	Functionalized linker to form high-symmetry adsorption sites in micropore COF for CO2 capture and separation: insight from GCMC simulations. Journal of Materials Science, 2022, 57, 6282-6292.	3.7	8
83	<i>In Situ</i> Growth of MOF-Derived NaCoPO ₄ @Carbon for Asymmetric Supercapacitive and Water Oxidation Electrocatalytic Performance. Nano, 2019, 14, 1950148.	1.0	7
84	Precise regulation of CO2 packing pattern in s-block metal doped single-layer covalent organic frameworks for high-performance CO2 capture and separation. Chemical Engineering Journal, 2022, 441, 135903.	12.7	7
85	Phosphate Group Dependent Metallic Co(OH) ₂ toward Hydrogen Evolution in Alkali for the Industrial Current Density. ACS Sustainable Chemistry and Engineering, 2022, 10, 7100-7107.	6.7	7
86	A facile approach to fabricate superhydrophobic and corrosion resistant surface. Materials Research Express, 2015, 2, 015501.	1.6	5
87	One-dimensional isomeric and hierarchical TiO ₂ nanostructures: novel air stable semiconducting building blocks. Journal of Materials Chemistry C, 2013, 1, 213-215.	5.5	4
88	In situ thermolysis of Pt-carbonyl complex to form supported clean Pt nanoclusters with enhanced catalytic performance. Science China Materials, 2017, 60, 131-140.	6.3	4
89	Synergistic doping and tailoring: Realizing in depth modulation on valence state of CoFe spinel oxide for high-efficiency water oxidation. Applied Surface Science, 2022, 572, 151388.	6.1	4
90	Multi-objective optimization of alkali/alkaline earth metals doped graphyne for ultrahigh-performance CO2 capture and separation over N2/CH4. Materials Today Physics, 2021, 21, 100539.	6.0	4

#	Article	IF	CITATIONS
91	Synthesis of AgInS2-xAg2S-yZnS-zIn6S7 (x, y, z = 0, or 1) Nanocomposites with Composition-Dependent Activity towards Solar Hydrogen Evolution. Materials, 2016, 9, 329.	2.9	3
92	Theoretical investigation on two-dimensional conjugated aromatic polymer membranes for high-efficiency hydrogen separation: The effects of pore size and interaction. Separation and Purification Technology, 2022, 299, 121674.	7.9	1
93	Status and Perspectives on the Photocatalytic Reduction of CO ₂ . World Scientific Series in Nanoscience and Nanotechnology, 2016, , 229-288.	0.1	0
94	Theoretical Investigation of the Fusion Process of Mono-Cages to Tri-Cages with CH4/C2H6 Guest Molecules in sl Hydrates. Molecules, 2021, 26, 7071.	3.8	0